BIOCHEMISTRY
including biophysical chemistry & molecular biology
Article

Biochemistry **2010,** *49,* 6557–6566 6557
DOI: 10.1021/bi100362k

Zebrafish (*Danio rerio*) Endomembrane Antiporter Similar to a Yeast Cation/H^+ Transporter Is Required for Neural Crest Development[†]

Murli Manohar,[‡,⊥,▽] Hui Mei,[‡,▽] Andrew J. Franklin,[#] Elly M. Sweet,[§] Toshiro Shigaki,[⊥] Bruce B. Riley,[§] Colin W. MacDiarmid,[∥] and Kendal Hirschi*[,‡,⊥]

[‡]*Vegetable and Fruit Improvement Center, Texas A&M University, College Station, Texas 77845,* [§]*Department of Biology, Texas A&M University, College Station, Texas 77843,* [∥]*Department of Nutritional Sciences, University of Wisconsin—Madison, Madison, Wisconsin 53562,* [⊥]*United States Department of Agriculture/Agricultural Research Service, Children's Nutrition Research Center, Baylor College of Medicine, Houston, Texas 77030, and* [#]*Department of Surgery, Washington University School of Medicine, St. Louis, Missouri.* [▽]*These authors contributed equally to this work.*

Received March 9, 2010; Revised Manuscript Received June 7, 2010

ABSTRACT: CAtion/H^+ eXchangers (CAXs) are integral membrane proteins that transport Ca^{2+} or other cations by exchange with protons. While several yeast and plant CAX proteins have been characterized, no functional analysis of a vertebrate CAX homologue has yet been reported. In this study, we further characterize a CAX from yeast, VNX1, and initiate characterization of a zebrafish CAX (Cax1). Localization studies indicated that both Vnx1 and Cax1 proteins are found in endomembrane compartments. Biochemical characterization of endomembrane fractions from vnx1 mutant cells and zebrafish Cax1-expressing yeast cells suggested that both yeast and fish CAXs have Ca^{2+}/H^+ antiport activities. Additionally, the vnx1 mutation was associated with heightened pH-sensitivity. In zebrafish embryos, cax1 was specifically expressed in neural crest cells. Morpholino knockdown of cax1 caused defects in neural crest development, including alterations in pigmentation, defects in jaw development, and reduction in expression of the neural crest marker, Pax7. Collectively, our findings provide insights into Vnx1 function and support an unexpected role of CAX transporters in animal growth and development.

Calcium ion (Ca^{2+}) is a ubiquitous second messenger in signal transduction pathways regulating many physiological and developmental processes (*1*−*3*). Ca^{2+} concentrations are maintained by transmembrane Ca^{2+} fluxes mediated by Ca^{2+} transporters located in both the plasma membrane and endomembranes. Analysis of the growing volume of genomic sequence data from a variety of species suggests many as-yet-uncharacterized proteins may contribute to transport of Ca^{2+} during growth and development.

In yeast and plant cells, CAtion/H^+ eXchanger (CAX[1]) proteins have been identified as playing a role in the restoration of low cytosolic Ca^{2+} levels after Ca^{2+} signaling events (*4*−*6*). CAX proteins use a proton gradient generated by proton pumps to export Ca^{2+} or other cations from the cytosol (*7*). There are nearly 200 CAX open reading frame (ORF) sequences available in public sequence databases. Phylogenetic analysis of these proteins indicated that the CAX family consists of three major groups (Types I, II, and III) (*8*). Several Type I and Type III CAXs have been well characterized, including Vcx1 from yeast and *Escherichia coli* ChaA (*4*, *5*, *9*−*13*). When compared to Type I and III CAXs, Type II CAXs have a unique N-terminal secondary structure and two or more additional transmembrane (TM) domains at the N-terminus. To date, the only Type II CAX that has been functionally characterized is Vnx1 from the yeast *S. cerevisiae* (*14*). A *vnx1* mutant was shown to exhibit lower activity of a Na^+/H^+ exchanger in vacuole membranes, and when combined with other mutations inactivating Na^+ transport systems, the *vnx1* mutation conferred slightly higher sensitivity to Na^+ ions. However, the apparent minor contribution of Vnx1 to sodium homeostasis suggests that vacuolar sodium transport may not be the sole physiological role of this protein.

The function of CAX proteins has been primarily studied in plant, bacterial, and fungal systems. Reports have speculated that H^+-dependent Ca^{2+} transporters are not found in animal cells (*15*). However, genome sequence analysis has identified members of the Type II CAX subgroup in a broad range of organisms, including animals such as *Xenopus*, sea urchins, and fish species (*8*). Little is known about the biochemical function or physiological role of these animal Type II CAX proteins.

Zebrafish (*Danio rerio*) has emerged as a powerful model for dissecting the relationship between Ca^{2+} signaling and development (*1*, *16*, *17*). Ca^{2+} signaling plays crucial roles in developmental processes ranging from the initiation of fertilization to embryonic patterning and organogenesis (*18*). Ca^{2+} signaling mediates the induction and establishment of the highly migratory pluripotent neural crest cells that give rise to a variety of differentiated cell types, such as cranial cartilage, neurons, and pigment cells (*19*−*21*). The Ca^{2+} signaling process directing neural crest cell migration and differentiation has been extensively studied, but the transporters involved in

[†]This work was supported in part by the U.S. Department of Agriculture/Agricultural Research Service (under Cooperative Agreement 58−62650−6001), the National Science Foundation (NSF; grant nos. 0344350), and the U.S. Department of Agriculture Grant CSRESS#2005−34402−16401 Designing Foods for Health.

*To whom correspondence should be addressed. Phone: (713) 798-7039. Fax: (713) 798-7171. E-mail: kendalh@bcm.edu.

[1]Abbreviations: CAXs, CAtion/H^+ eXchangers; TM, transmembrane; hpf, hours postfertilization; HA, hemagglutinin; GPD, glyceraldehyde phosphate dehydrogenase; TB, translation blocker; SB, splice blocker; MO, morpholino; ALP, yeast vacuolar alkaline phosphatase.

Published on Web 06/25/2010

Ca^{2+} transport and distribution to regulate the intracellular Ca^{2+} concentration have been less well understood. Zebrafish CAX homologues may serve as valuable tools to dissect the function of animal CAX transporters in growth and development.

In this article, we describe further characterization of the yeast type II CAX, Vnx1, and report the cloning and characterization of zebrafish *cax1*, encoding a vertebrate Type II CAX. We examined the subcelluar localization and biochemical function of both Vnx1 and zebrafish Cax1 proteins. The developmental phenotypes of zebrafish embryos with reduced *cax1* expression suggested that its function may be required for neural crest development. We propose that type II CAXs are predominantly endomembrane localized transporters involved in both pH regulation and ion homeostasis.

MATERIALS AND METHODS

Phylogenetic Analysis. A phylogenetic analysis was performed on the 28 full length Type II CAX sequences from the public databases. The sequences were obtained by performing BLASTP against the reference sequence Vnx1p (accession no. DAA10241) on April 15, 2010 using the National Center for Biotechnology Information BLAST Web site (http://blast.ncbi.nlm.nih.gov/Blast.cgi). Multiple sequence alignments were performed using ClustalW, available on the European Bioinformatics Institute Web site (http://www.ebi.ac.uk/clustalw/), with additional manual adjustments. Only the homologous regions were used for the multiple sequence alignments. The phylogenetic tree on the data sets was constructed using Protdist and Fitch programs in the phylogenetic suite Phylip (*22*). The tree file was visualized by the program Treeview (*23*).

Yeast Techniques. Basic yeast culture conditions and transformation procedures were described in previous studies (*24*, *25*). Briefly, yeast cells were transformed using the lithium acetate/single-stranded carrier DNA/polyethylene glycol method and selected on synthetic complete medium lacking uracil. To determine tolerance to low pH conditions, a synthetic phosphate-buffered minimal medium was prepared as previously described (*26*). The pH was adjusted to the required value using phosphoric acid.

Plasmid and Strain Construction. The Cax1 and HA-Cax1 clones were subcloned into the yeast expression vector piHGpd (*27*) as described in previous studies (*24*). pFL44YNL was constructed via homologous recombination between a *VNX1* PCR product generated using the oligonucleotides YNL321wF (5′-CGTTGTAAAACGACGGCCAGTGAATTCGAGCTATGTAATAGCGTGCGACG-3′) and YNL321wR (5′-GACCATGATTACGCCAAGCTTGCATGCCTGCACAGTGCAATTGACGGAGA-3′) and the pFL44-S plasmid (*28*). pFL44HAYNL was constructed by amplifying a *VNX1* PCR product with the YNL321wF and YNL3xHA-tag oligonucleotides, followed by replacement of the *ZRC1* gene in YEpZRC1-HA (*29*) via homologous recombination. 211YNL44 was constructed via homologous recombination between pFL44YNL and a YFP PCR product amplified from pKT211 (*30*) using the oligonucleotides 5′ universal FP 5′-TATTGTTGTAGGATTCTACTTCCAGGGAGCTCTTTCGGAGGACGGTGCTGGTTTAATT-3′) and 3′ universal FP (5′-ATTGGTAGGTATCCAGGTGAAAAGCGGGGACAGTTGCTTTCCACTAGTGGATCTGATA-3′). The pynl321w::LEU2 plasmid was constructed by replacing part of the *VNX1* coding sequence in pFL44YNL with the *LEU2* gene via homologous recombination. *LEU2* was amplified from DY1457 genomic DNA using the oligonucleotides 5′ leu2 (5′-TTTAGAGCACCACCGCACATGGACAGACCTGGAGCAGATCTGGTACTTTG-3′) and 3′ leu2 (5′-ATTAGTATGCAGCAATTCTACAATTGGGTGACGCCAGCAGATCTATTACA-3′). To construct a vector for transfection of cultured cells, a full-length *cax1* cDNA was inserted between *Xho*I and *Eco*RI sites of the pEGFP-C1 vector (Clontech).

Yeast *vnx1* deletion mutants (Δ*vnx1*) were generated by replacing the *VNX1* ORF in W303-1A, K661, K665, and K667 (*31*) with the KanMx6 gene using a PCR-based deletion method (*32*). The genetic background of K661 (Δ*vcx1*), K665 (Δ*vcx1 pmc1*::*TRP1*), and K667 (Δ*vcx1 cnb1*::*LEU2 pmc1*::*TRP1*) was W303-1A (*MAT***a** *ade2-1 can1-100 his3-11,15 leu2-3,112 trp1-1 ura3-1*). A PCR product was generated using the following primers: YNL321w-F1 5′ ATATACAAGTGCTTAATTCTTGATTTTTATTTTCCGTACGCTGCAGGTCGAC-3′ and YNL321w-R1 5′-GGATACTTTATACTAATAATTGACATTTCTATCGATCGATGAATTCGAGCTCG-3′, and correct disruption was verified by PCR. A Δ*vnx1* Δ*pmr1* strain was generated by crossing Δ*vnx1* to K610 (*pmr1*::*HIS3*, isogenic to W303-1A) (*4*). AJF02 (*MATa ade6 can1-100*^{oc} *his3-11,15 leu2-3,112 trp1-1 ura3*−*52 ynl321w*::*LEU2*) was constructed by the transformation of DY1457 (*33*) with plasmid pynl321w::LEU2. AJF16 (*MATa ade6, can1-100oc, his3-11,15 leu2 trp1-1 ura3 nhx1*::*TRP1 ynl321w*::*LEU2*) was constructed by crossing AJF02 and WX1 (*MAT*α *leu2-13 112 ura3-1 trp1-1 his3-11, 15 ade2-1 can1-100 nhx1*::*TRP1*) (*34*). Metal tolerance assays were performed by growing yeast at 30 °C for 3 days on SC medium supplemented with appropriate metals.

ICP-AES Analysis of Yeast Elemental Content. Yeast cultures were inoculated in 5 mL of yeast−peptone−dextrose (YPD) and 1/100 vol. of 100× mineral supplement stock (*25*) supplemented with 10 mM $CaCl_2$. The cells were grown at 30 °C to stationary phase. A 2.5 mL sample of each culture was collected by vacuum filtration using isopore membrane filters (1.2 μm pore size) (Fisher Scientific, Pittsburgh, PA, USA). Cells were washed three times with 1 mL of 1 μM ethylenediaminetetraacetic acid disodium salt solution, pH 8.0, by vacuum filtration followed by three washes with 1 mL of distilled, deionized H_2O. The filters were dried at 70 °C in an oven for 48 h before inductively coupled plasma atomic emission spectroscopy (ICP-AES) analysis was performed as previously described (*35*). Final concentrations were normalized to cell density.

Cell Culture and Transfection. HeLa and HEK293 cells were cultured in improved minimal essential medium (Mediatech, Herndon, VA). Each medium was supplemented with 2 mM glutamine, 1× antibiotic−antimycotic cocktail, and 10% heat-inactivated fetal bovine serum (Invitrogen). All cells were maintained at 37 °C in 5% CO_2. One microgram of plasmid DNA was used for transfection.

Fluorescence Microscopy. Hela cells were grown on glass coverslips coated with poly-D-lysine, fixed in 4% paraformaldehyde, and mounted in medium containing the chromatin stain 4′,6′-diamidino-2-phenylindole (DAPI; Molecular Probes). Slides were viewed by using a Zeiss Axiovert microscope deconvolution microscopy system with a Zeiss 100× (1.4 numerical aperture) oil immersion lens. Z sections were collected at an optical depth of 0.25 μm and images optimized using Zeiss deconvolution software. To image YFP in live yeast cells, cultures were grown to log phase in standard synthetic medium lacking uracil, harvested by centrifugation, and mounted on

polylysine-coated microscope slides. Images were captured using a Zeiss Axioscope microscope.

Cell Fractionation. For Western analysis and $^{45}Ca^{2+}$ transport assays, microsomal membranes were prepared from yeast expressing HA-Cax1 (Figure 4) as described previously (*24*). Protein concentrations were determined by using the Bio-Rad protein assay (Bio-Rad, Hercules, CA). Immunoblots were performed, and the HA epitope was detected by anti-HA monoclonal primary antibody obtained from Abcam Inc. (Cambridge, MA) and yeast organelle monoclonal primary antibody obtained from Molecular Probes (Eugene, OR) essentially as described previously (*24*). Sucrose gradient cell fractionations for Vnx1 localization (Figure 2) were performed essentially as previously described (*36*). Calcium transport in sucrose gradient fractions was assayed as previously described (*37*). To quantify proton gradient-dependent activity, assays were performed in the presence and absence of 25 μM carbonyl cyanide *m*-chlorophenylhydrazone (CCCP) (a protonophore, which disrupts the proton gradient across the lipid bilayer membrane), and 10 nM bafilomycin A (V-ATPase inhibitor), and the former values subtracted from the latter to obtain the activity shown.

Fish Strains. The wild-type strain was derived from the AB line (Eugene, OR). Embryos were developed at 28.5 °C in fish water containing meythlene blue and staged according to standard criteria (*38*). Fish were housed on a recirculation system approved by Institutional Animal Care and Use Committee (IACUC) and University Laboratory Animal Care Committee (ULAC).

Morpholino Injections. Morpholino oligomers obtained from Gene Tools Inc. (Philomath, OR) were diluted and injected as previously described (*39*, *40*). Unless stated otherwise, at least 25 specimens were examined for each experiment. To knockdown *cax1*, 7.5 ng of either translation-blocking morpholinos or splice-blocking morpholinos were injected per embryos. *cax1*-MO sequences are as follows: *cax1* translational blocking MO, 5′-ACATCGTGGGTTTGATTTGAGCCAT-3′; *cax1* splice blocker exon1/2 (splice donor site), 5′-AGATGATTATAATACTGACCTGAGC-3′; *cax1* splice blocker exon2/3 (splice acceptor site), 5′-CTTAAATACTCACTGTGGGCAGAGA-3′. In most experiments, embryos were also injected with a p53-MO to block nonspecific cell death (*41*).

In Situ Hybridization and Alcian Blue Staining. *In situ* hybridization was carried out as described previously (*40*). The 1.6 kb and 0.3 kb *cax1* N-terminal coding sequences were cloned into the pCRII-TOPO vector (Invitrogen), and a *cax1* RNA probe was transcribed using SP6 RNA polymerase. Antisense riboprobes were transcribed from plasmids containing *Drcax1*. Embryo staining with Alcian blue was performed as previously described (*42*, *43*).

Mis-Expression of Drcax1. A full-length *cax1* cDNA was cloned into the pCS2 expression vector to generate the vector pCS2-*cax1* vector. RNA was synthesized *in vitro* from the pCS2-*cax1* plasmid using the mMessage mMachine kit (Ambion, Austin, TX), and 200−300 ng of *cax1* RNA was injected into the yolk of cleaving embryos at the one-cell stage. In some experiments, *cax1* mRNA was coinjected with *cax1* MO. To misexpress *cax1* under the control of the cytomegalovirus promoter, 30−60 pg of plasmid DNA was injected into one-cell embryos or was coinjected with *cax1* splice blocker exon 2/3 MO.

Immunostaining of Zebrafish Embryos. Antibody staining was performed as described previously (*43*). Embryos were incubated with the primary monoclonal antibody Pax7 (1:150) purchased from the Developmental Studies Hybridoma Bank (Iowa City, IA). Embryos were washed and incubated with horseradish peroxidase-conjugated goat antimouse IgG (Vector Laboratories, Burlingame, CA; diluted 1:200).

RESULTS

Identification of Zebrafish cax1. To study the function of a vertebrate Type II CAX, we set out to clone zebrafish *cax1* using a PCR-based approach. Microarray data suggest that zebrafish *cax1* is expressed in reproductive organs during development and later in the adult kidney with highest levels of expression occurring in embryos 24 hpf (hours postfertilization). Therefore, total RNA was extracted from zebrafish 24 hpf embryos and used to amplify the *cax1* full length cDNA using gene-specific primers. The *cax1* cDNA was 2,295 nucleotides in length and encoded a 764 amino acid polypeptide (accession no. DQ631793, Figure 1). The deduced protein was aligned with previously identified yeast Type II CAX, Vnx1, and other animal Type II CAXs (Figure 1). Zebrafish Cax1 was only 28% identical (33% similarity) to Vnx1 and exhibited much higher identity to other animal Type II CAXs. It is 66% identical (77% similarity) to another Type II CAX in the zebrafish genome (Cax2), 62% identical (76% similarity) to *Xenopus* Type II CAX, and 64% identical (77% similar) to fugu (*Fugu rubripes*) Type II CAX (data not shown).

All full-length Type II CAX sequences except those of Ascomycetous fungi were analyzed for phylogenetic relationships. Because there are numerous Type II CAX sequences from Ascomycetous fungi species, only nine (including the reference sequence) were included in the analysis. The Type II CAX proteins have a relatively restricted phylogenetic distribution, members being only from five major taxonomic groups (animals, slime molds, protozoa, Ascomycetous fungi, and Basidiomycetous fungi), although this may simply reflect the paucity of genomic information from other taxa. The phylogenetic tree demonstrated that each of the five major groups formed a well-defined clade. Most species contained one copy of a Type II CAX, although some species, such as zebrafish (*Danio rerio*), *Polysphondylium pallidum*, *Trichomonas vaginalis*, and *Vanderwaltozyma polyspora*) contained two dissimilar sequences (Figure 1).

Subcellular Location of Vnx1 in Yeast. To initiate biochemical studies of zebrafish Cax1 via heterologous expression in yeast, we required a yeast strain that did not express endogenous calcium/proton exchangers. Previous studies of yeast calcium transporters revealed that at least two major activities are present in yeast cells. In addition to Vcx1-dependent activity, a second calcium/proton exchange activity has been observed, the activity of which was enhanced in a Δ*pmr1* strain (*12*). The authors suggested that this residual exchanger activity might be contributed by the Vnx1 (Ynl321w) protein. If Vnx1 does perform this function, it would be expected to be located within an endomembrane compartment distinct from the vacuolar membrane (*12*). However, a previous study concluded that a version of Vnx1 with a centrally inserted epitope tag was located in the vacuolar membrane (*14*). In addition, this study suggested that Vnx1 was required for the expression of a sodium/proton exchange activity in the vacuole membrane, implying a direct role for Vnx1 in sodium transport. Because to date the majority of functionally characterized CAX proteins have been implicated in calcium transport (*44*), and Δ*vcx1* cells still displayed residual CAX activity (*12*), we decided to reinvestigate the contribution of Vnx1 to calcium transport.

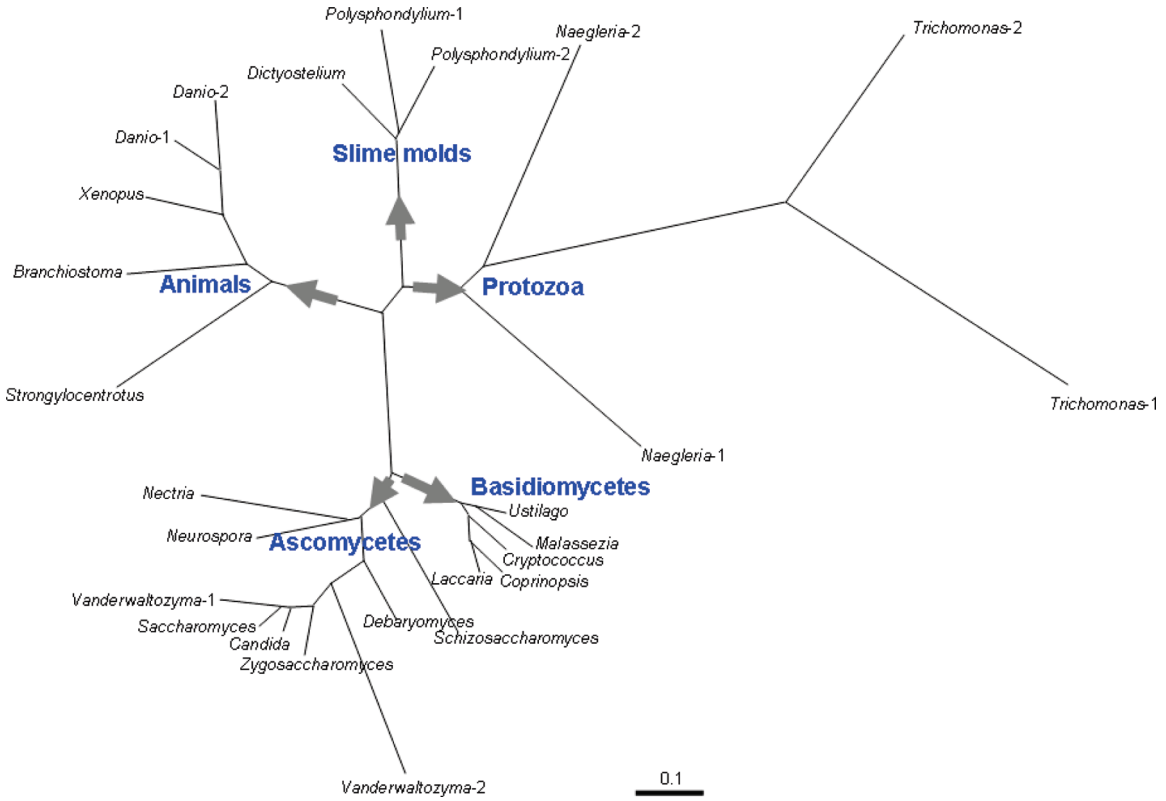

FIGURE 1: Alignmentof all full-length Type II CAX sequences except those of Ascomycetous fungi. The tree branches are labeled with the species from which each CAX was derived. When there are multiple CAXs from the same species, they are distinguished by a number after the specific epithet. The GenBank accession numbers of all sequences are available as Supporting Information online.

To determine if Vnx1 could contribute to Ca^{2+}/H^+ exchange in a nonvacuolar compartment (*12*), we determined the location of epitope-tagged Vnx1 in yeast. To increase the relatively low expression level of Vnx1 and allow its detection by immunoblotting, a C-terminal epitope-tagged version of Vnx1 (Vnx1-HA) was constructed in a multicopy (2 μ) plasmid. In Western blots of total protein from strains expressing Vnx1-HA, the protein was detected as two forms, one with an apparent molecular weight of approximately 100 kDa (similar to the predicted molecular weight for Vnx1-HA of 102.5 kDa), and one of a size too large to be accurately estimated by SDS−PAGE. The abundance of this larger form was reduced when the SDS concentration in the gel-loading buffer was increased, suggesting that it represented an SDS-resistant complex (data not shown). Organelle fractionation revealed that Vnx1-HA was relatively broadly distributed through the fractions of the sucrose gradient. However, the protein was predominately found in heavier fractions of the gradient, where its distribution overlapped with the ER-associated protein Dpm1 (Figure 2A). Although it appeared that a small amount of the protein may be present in other compartments (for example, the Golgi, prevacuolar compartment, and vacuole), these results suggested that Vnx1-HA associated with the ER membrane.

To verify this observation using an independent method, we also examined the distribution of a Vnx1-YFP fusion protein in yeast. As shown in Figure 2B, cells expressing Vnx1-YFP displayed a distinct fluorescent signal outlining the nucleus (visible as a slight depression in the DIC images), while control cells showed only diffuse autofluorescent background. In some Vnx1-YFP cells, an additional minor fluorescent signal was observed around the periphery of the cell. These patterns are consistent with an ER membrane location for Vnx1. Thus, both cell fractionation and epifluorescence studies indicated that the Vnx1 protein is concentrated in the ER membrane, consistent with this protein contributing to Ca^{2+}/H^+ exchange in an endomembrane compartment.

Effect of the Δvnx1 on Calcium Transport and Elemental Content. Recent advancements in mass spectroscopy have made it possible to accurately survey the elemental content of yeast and plant tissues (*35*). When factors important for nutrient homeostasis are genetically ablated, the resulting alterations in this profile can provide evidence for gene function (*25*, *44*, *45*). As previously noted, a Vcx1-independent Ca^{2+}/H^+ transport activity was observed in yeast cells deficient in Golgi Ca^{2+}-ATPase Pmr1 (*12*). To determine if this Ca^{2+}/H^+ exchange activity was dependent on Vnx1, we constructed a Δ*vnx1*Δ*pmr1* double mutant strain. We then used sucrose gradient cell fractionation to isolate endomembrane-enriched fractions lacking vacuolar membranes from Δ*pmr1* single and Δ*vnx1* Δ*pmr1* double mutant strains, and measured the proton-gradient dependent Ca^{2+} transport activity in these fractions. In the Δ*pmr1* single mutant strain, robust Ca^{2+}/proton exchange activity was observed, but this activity was almost eliminated in Δ*vnx1*Δ*pmr1* mutant cells (Figure 4B). This observation is consistent with Vnx1 contributing to calcium transport within an endomembrane compartment distinct from the vacuole.

To further characterize the physiological role of Vnx1, we used ICP-AES to determine the elemental profile of WT and Δ*vnx1* yeast strains. Under normal conditions, elemental content of Δ*vnx1* was similar to those of Δ*pmc1*, Δ*vcx1* and wild type cells (data not shown). When Vnx1, Vnx1-HA, and Vnx1-YFP were expressed in yeast cells, they all mediated an increase in Mn^{2+} content (Supporting Information, Figure 2) as well as an increase in Mg^{2+} content in the Vnx1 and Vnx1-HA overexpressing strains

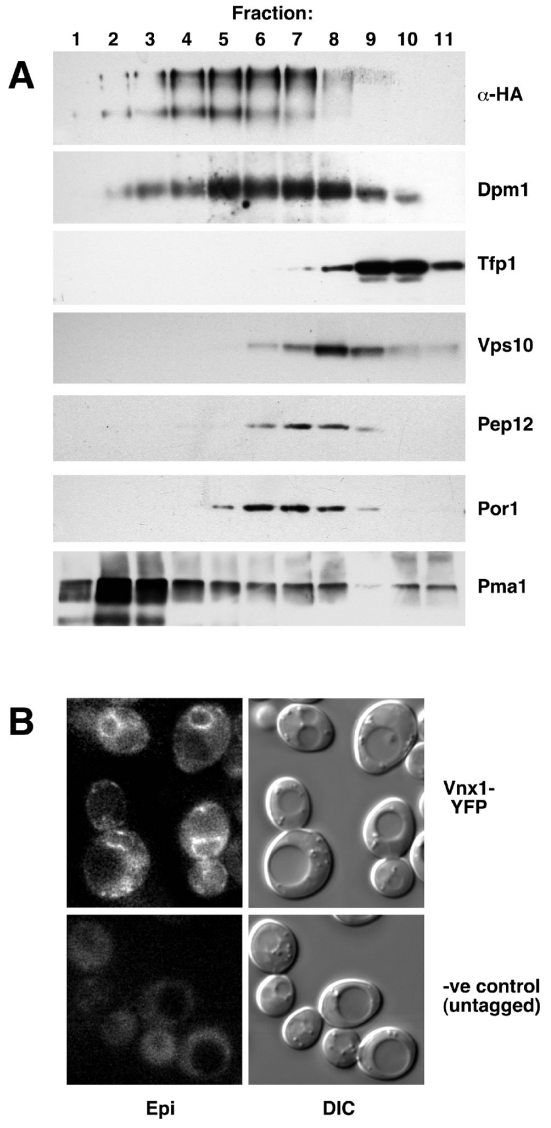

FIGURE 2: Subcellular location of Vnx1 in yeast. (A) Localization of Vnx1 by cell fractionation. Organelles were isolated from DY1457 transformed with pFL44YNLHA and fractionated on Mg^{2+}-free sucrose gradients. Equal volumes of each fraction were separated by SDS−PAGE and subjected to Western blotting with α-HA (Vnx1-HA; MW ~100 kDa), α-Dpm1 (ER; MW ~30 kDa), α-Tfp1 (vacuole; MW ~118 kDa), α-Vps10 (Golgi; MW ~180 kDa), α-Pep12 (early endosome; MW ~33 kDa), α-Por1 (mitochondria; MW ~30 kDa), and α-Pma1 (plasma membrane; MW ~100 kDa) monoclonal antibodies. (B) Visualization of Vnx1-YFP by epifluorescence microscopy. A diploid yeast strain (BY4743) was transformed with 211YNL44YFP (Vnx1-YFP) and grown to log phase in synthetic medium. YFP (Epi) and DIC images were obtained. Negative control cells (untagged) were transformed with pFL44YNL.

(Supporting Information, Figure 3). This observation suggests that the tagged transporters were functional and that Vnx1 plays a role in cation homeostasis.

Ca^{2+} homeostasis in yeast is controlled in part by the action of Pmc1, a vacuolar Ca^{2+} ATPase, and Vcx1, a vacuolar Ca^{2+}/H^+ that is regulated by calcineurin. Inactivation of these factors confers increased Ca^{2+} sensitivity to yeast (*4*). To determine if Vnx1 also contributed to Ca^{2+} tolerance, we constructed strains with combinations of mutations in these factors, including Δ*vnx1*Δ *vcx1,* Δ*vnx1* Δ*vcx1* Δ*pmc1*, and Δ*vnx1* Δ*vcx1* Δ*pmc1* Δ*cnb1* (the Δcnb1 mutation inactivates calcineurin). However, we failed to observe a significant change in calcium tolerance associated with the Δ*vnx1* mutation in any of these genetic backgrounds. In addition, we observed no effect of the Δ*vnx1* mutation on tolerance to other toxic metals.

Effect of the Δvnx1 Mutation on pH Sensitivity. Previous studies of Vnx1 implicated this protein in sodium/proton exchange in the vacuolar membrane. However, it is unclear as to how much of a contribution Vnx1 makes to sodium homeostasis. The effect of the Δ*vnx1* on sodium tolerance was minor (*14*), and we noticed no clear increase in sensitivity to any divalent or monovalent cations associated with the Δ*vnx1* (including calcium and sodium; data not shown). In addition, the overexpression of Vnx1 in yeast did not alter sodium accumulation or tolerance, even when present at high extracellular concentrations (data not shown). Some yeast cation exchangers have been shown to be required for both metal ion homeostasis and regulating the pH of cytosolic and organelle compartments. For example, the Nhx1 protein is required both for function of the endosomal compartment in yeast and for cytosolic pH homeostasis. The Δ*nhx1* strain displays lower pH in the vacuolar lumen and cytosolic compartment, and a growth defect in low pH conditions (*26*). To test if Vnx1 might contribute to pH regulation, we constructed strains with one or both of these mutations, then tested their effect on tolerance to low pH. Although the Δ*nhx1* was associated with a slight growth defect, the *vnx1* mutation had little effect in isolation. However, the double mutant strain had an enhanced sensitivity to low pH, indicating a synthetic interaction of the Δ*vnx1* and Δ*nhx1* (Figure 3B). This observation suggests that both Nhx1 and Vnx1 may contribute to the regulation of intracellular pH.

Functional Characterization of Zebrafish Cax1 by Heterologous Expression. To perform a preliminary biochemical characterization of zebrafish Cax1, an epitope-tagged variant was generated by fusion of three repeats of the HA (hemagglutinin) epitope to the N-terminal end (designated HA-Cax1). To drive high-level expression in yeast, HA-Cax1 was fused to the promoter of the constitutive glyceraldehyde phosphate dehydrogenase gene (*GPD1* (*25*)). To test the function of HA-Cax1, we expressed both the untagged and tagged protein in Δ*vnx1* cells and quantified elemental content in Ca^{2+} containing media using ICP-AES. Calcium content of *vnx1* cells expressing either version of zebrafish Cax1 increased 2-fold when compared with the vector-only control (Figure 3A). Two conclusions can be drawn from these observations; first, zebrafish Cax1 can function to yeast Ca^{2+} sequestration; and second, that the HA-tag did not inhibit Cax1 function. Using the HA-tagged version of zebrafish Cax1, we performed cell fractionation experiments to determine the location of the protein in yeast cells (Figure 4A). HA-Cax1 was detected in fractions that overlapped with an ER marker protein. To characterize the effect of zebrafish Cax1 expression on calcium transport, we isolated suitable fractions of yeast organelles for assays of proton-gradient dependent calcium accumulation (Figure 4B). For these experiments, Cax1 was expressed in a Δ*vnx1* Δ*pmr1* double mutant strain lacking endomembrane-associated Ca^{2+}/H^+ exchange activity. On the basis of cell fractionation results, we attempted to use vacuole membrane-free fractions to perform calcium transport assays. When expressed in Δ*vnx1* Δ*pmr1 cells*, Cax1 restored endomembrane proton-gradient-dependent transport activity to a level similar to that observed in membranes of the Δ*pmr1* strain (Figure 4B). This result supports a role for Vnx1 in proton-gradient-dependent calcium transport.

Subcellular Location of Zebrafish Cax1. To determine the location of zebrafish Cax1 in animal cells, a GFP-tagged version

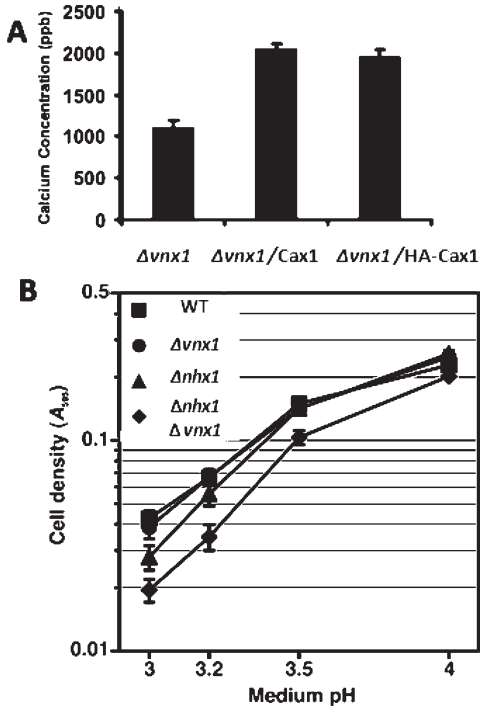

FIGURE 3: (A) Vector-, Cax1-, and HA-Cax1 expressing Δ*vnx1* yeast cells were grown in yeast−peptone−dextrose (YPD) medium with mineral supplements and additional 10 mM $CaCl_2$. Data represent the means (±SEM) of three independent analyses. (B) Effect of Δ*vnx1* and Δ*nhx1* mutations on yeast pH tolerance. Phosphate-buffered synthetic medium adjusted to the indicated pH was inoculated with cells of the indicated genotypes (DY1457, Δ*nhx1*, Δ*vnx1*, and Δ*nxh1* Δ*vnx1*) to an initial A_{595} of 0.01. After 16 h of growth, A_{600} was determined. Data points indicate the mean of three independent experiments; error bars = ± SEM.

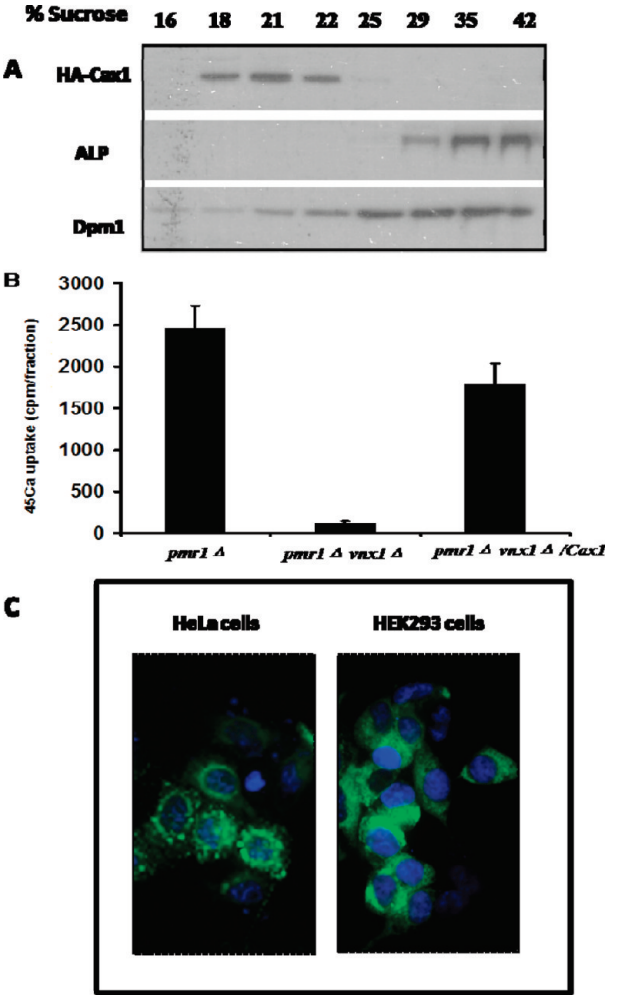

FIGURE 4: Ca^{2+}/H^+ antiport activity in Δ*pmr1*, Δ*vnx1* Δ*pmr1*, and Δ*vnx1* Δ*pmr1*/*cax1* yeast. (A) W303 was transformed with HA-Cax1, grown to log phase, and organelles fractionated on a 15−48% sucrose gradient. An equal volume of each fraction was separated by SDS−PAGE and transferred to nitrocellulose. Proteins were detected with antibodies specific for the hemagglutinin epitope (HA-Cax1, MW ~ 86 kDa), yeast vacuolar alkaline phosphatase (ALP, MW ~70 kDa), and yeast endoplasmic reticulum protein dolichol phosphate mannose synthase (Dpm1, MW ~30 kDa). (B) Proton gradient-dependent Ca^{2+} uptake activity in non- vacuolar fractions. Data shown are the mean (±SE) of four independent experiments. (C) Subcellular localization of Cax1. Human HeLa cells and HEK293 cells transfected with GFP-tagged zebrafish Cax1 (green). 4′,6′-Diamidino-2-phenylindole (DAPI) counterstain was used to visualize nuclei (blue).

of the protein was expressed in human HeLa cells and HEK293 cells. GFP-Cax1 fluorescence was concentrated near the nucleus but distributed widely throughout the cytoplasmic matrix (Figure 4C). The observation that both Vnx1 and zebrafish Cax1 localize to endomembrane compartments suggests functional overlap between the yeast and animal type II CAX proteins.

Zebrafish cax1 Is Expressed in Neural Crest Cells. To investigate the developmental role of zebrafish *cax1*, we first examined the expression pattern of *cax1* using whole mount RNA *in situ* hybridization. Two probes were used, one containing the 1.6 kb *cax1* N-terminal coding sequence and a second specific to *cax1* containing a 0.3 kb *cax1* N-terminal sequence. Both probes produced similar results (data not shown). Therefore, for subsequent studies, only the 1.6 kb probe was used (Figure 5). At 24 and 48 hpf, *cax1* mRNA was predominantly detected in neural crest cells (Figure 5). To test if *cax1* mRNA was exclusively expressed in the neural crest, we examined *cax1* expression in embryos blocked for neural crest formation by injecting morpholinos designed to reduce the expression of the transcription factor genes *tfap2a* and *tfap2c* that are required for neural crest formation (*46*). In these morphants, *cax1* expression was no longer detected at 24 hpf (Figure 5).

Zebrafish Cax1 Is Required for Normal Neural Crest Development. To investigate the effects of zebrafish cax1 disruption by antisense morpholino (MO)-mediated knockdown, we designed three different morpholinos, one to block the translation of *cax1* and two to block pre-mRNA splicing. The *cax1* translation blocker (TB) and *cax1* splice blocker 2 (SB2) morpholinos both affected neural crest development, although to differing degrees. SB2 produced the most severe defects in neural crest development (Figure 5 and 6). RT-PCR confirmed that SB2 reduced the expression of *cax1* mRNA (data not shown). Because embryos injected with *cax1* SB2-MO showed some cell death, a potential indicator of MO-mistargeting, embryos in all subsequent experiments were coinjected with p53-MO and *cax1* SB2-MO to suppress artifactual morpholino-induced apoptosis (*41*). In agreement with the expression of *cax1*, the phenotype of *cax1* morphants was specific to neural crest development. Neural crest cells give rise to a variety of different cell types and contribute to a number of zebrafish body structures, including elements of the jaw and the characteristic horizontal-stripe pigment pattern. At 30 hpf, the pigmentation of *cax1* morphants was significantly reduced (Figure 6), although by 48 hpf, this phenotype was less evident (data not shown). Disruption of *cax1*

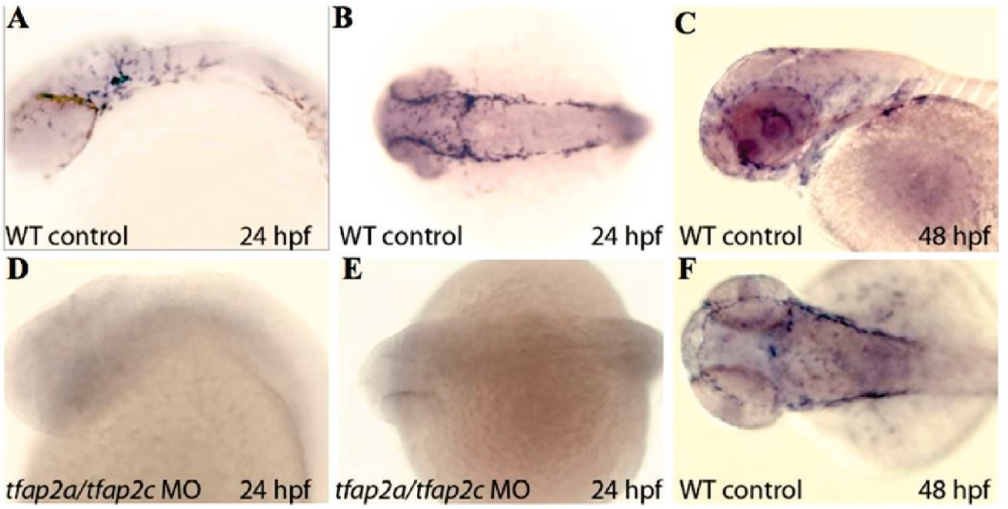

FIGURE 5: Expression of *cax1* in zebrafish embryos detected using *in situ* hybridization. A, D, and C show lateral views. B, E, and F show dorsal views. (A and B) Wild type embryos at 24 hpf showed *cax1* expression in neural crest cells. (C and F) Wild type embryos at 48 hpf showed low *cax1* expression in neural crest cells. (D and E) Embryos of tfap2a/tfap2c morphants at 24 hpf showed no *cax1* expression.

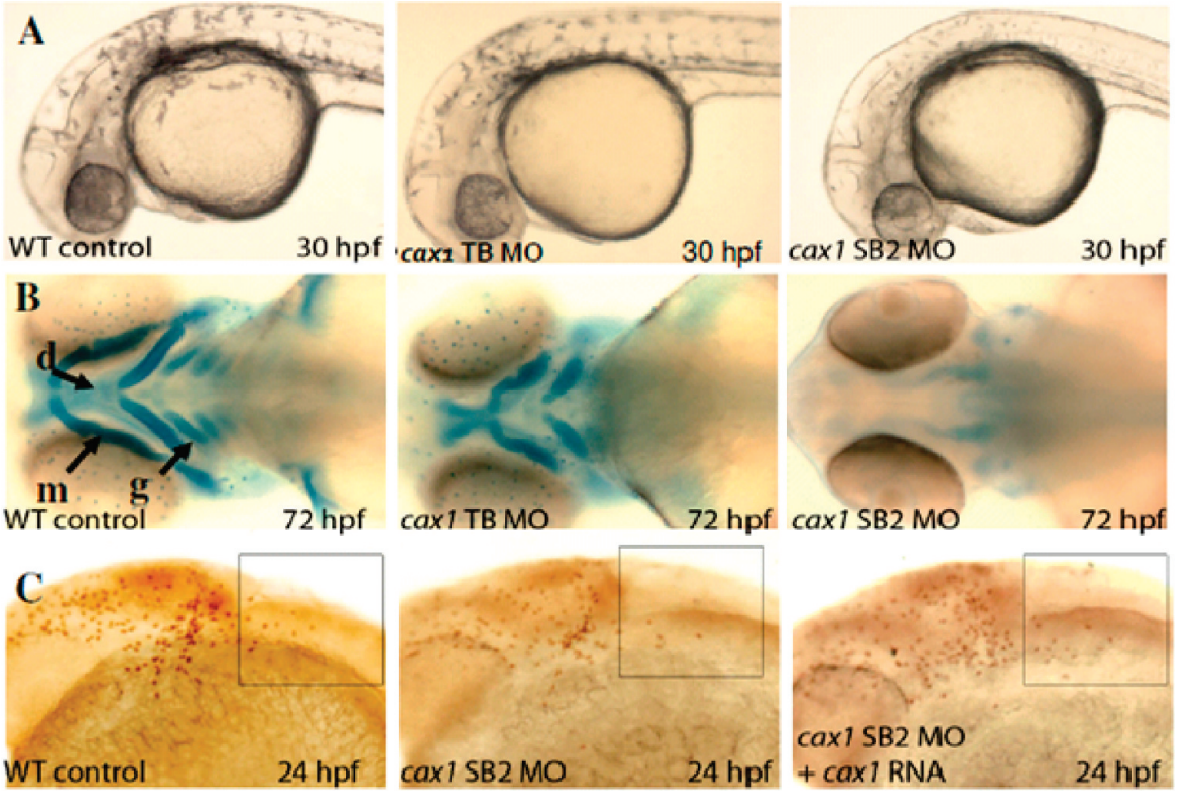

FIGURE 6: Impaired neural crest development in *cax1* morphants. (Panel A) The live image of 30 hpf embryos showed the slightly smaller head and reduced pigmentation in *cax1* morphants. (Panel B) Impaired neural crest development in *cax1* morphants. Alcian blue cartilage staining at 72 hpf in zebrafish embryos. Abbreviations: d, dorsal palate; g, gill arches; m, mandibular cartilage. Images show ventral views with anterior to the left. (Panel C) Anti-Pax7 staining at 24 hpf in embryos of a control, *cax1* morphants, and *cax1* morphants coinjected with *cax1* mRNA.

function also caused defects in jaw development, as seen by staining the jaw cartilage of 72 hpf embryos with Alcian blue (Figure 6). The gill arches, dorsal palate, and mandibular cartilages were absent or reduced in size in *cax1* SB2 morphants and to a lesser degree in *cax1* TB morphants. We also examined the expression of the neural crest marker, Paired box protein Pax7, in *cax1* morphants via the immunodetection of the Pax7 protein (*47*). At 24 hpf, there were fewer Pax7-expressing neural crest cells adjacent to the hindbrain in *cax1* morphants compared to that in the controls (Figure 6 and Table 1). This deficiency did not reflect a developmental delay as it could still be seen at 30 hpf (data not shown). The deficiency of Pax7-positive cells could be rescued by coinjecting either *cax1* mRNA or *cax1* plasmid DNA (Table 1). However, injecting 300 pg of *cax1* mRNA without MO coinjection also caused a reduction of Pax7-expressing neural crest cells, possibly reflecting nonspecific effects of excess *cax1* (data not shown). The defects in jaw cartilage in *cax1* morphants could not be rescued using either *cax1* mRNA or plasmid DNA (data not shown).

Table 1: Rescue of *cax1* Morphants by *cax1* DNA or mRNA Injections[a]

	no. of Pax7 expressing cells
control	8.8 ± 4.35 (n = 15)
cax1MO	4.4 ± 2.9 (n = 18) *P < 0.0001
control + cax1 RNA	4.9 ± 2.9 (n = 14) *P = 0.0014
cax1MO + cax1 RNA	10.25 ± 3.7 (n = 16) *P = 0.16 ‡P < 0.0001

	no. of Pax7 expressing cells
control	16.3 ± 4.7 (n = 12)
cax1MO	9.14 ± 5.3 (n = 18) *P < 0.0001
cax1MO + cax1 DNA	14 ± 4.1 (n = 16) *P = 0.05 ‡P = 0.0002

[a] P values are based on the t-test in comparison with the control (*) or with cax1MOs (‡).

DISCUSSION

A number of CAX family members from plants and microorganisms have been functionally characterized, but this study marks the first description of an animal CAX. While the phylogenetic distance between Vnx1 and zebrafish Cax1 suggests that their biological functions might have diverged during evolution, our studies suggest functional overlap still exists between animal and fungal type II CAX proteins. In this work, we demonstrate that yeast mutant cells lacking Vnx1 exhibit reduced activity of an endomembrane Ca^{2+}/H^+ exchange activity. The yeast and vertebrate proteins also exhibit other similarities suggestive of functional conservation, including localization to endomembrane compartments.

Although our results do not completely exclude Vnx1 function in other endomembrane compartments, the predominantly ER location of Vnx1 suggests that this protein directly or indirectly facilitates Ca^{2+}/H^+ exchange across the membrane of this organelle. Although the vacuole is the major store of calcium in yeast cells (*48*), the Golgi and ER compartments also contain a significant quantity of Ca^{2+} (*49*). In standard growth conditions, abolishing VNX1, VCX1, or PMC1 did not alter total Ca^{2+} content (data not shown) suggesting genetic buffering of Ca^{2+} content within the cells. The contribution of Vnx1 to calcium transport was most clearly observed in a *pmr1* mutant, which exhibited elevated activity of a Vcx1-independent Ca^{2+}/proton exchanger (*12*). Given its close relationship to known Ca^{2+}/H^+ exchangers, Vnx1 is the most likely candidate for this nonvacuolar exchange activity. The elevated activity of Vnx1 in the Δ*pmr1* cells may occur due to altered distribution or post-translational modification of Vnx1, as Δ*pmr1* mutants are known to exhibit defects in protein sorting and processing (*50*, *51*). It is possible that Vnx1 activity is tightly regulated and normally maintained at a low level in WT yeast but that this negative regulation is reduced in Δ*pmr1* cells. This effect could be due to the missorting of Vnx1 to a compartment missing a regulatory partner or as a consequence of altered calcium homeostasis in *pmr1* cells, which exhibit increased cytosolic free Ca^{2+}. We speculate that the loss of Pmr1 activity results in a compensatory increase in Vnx1 activity in order to maintain cytosolic or organelle Ca^{2+} homeostasis.

A primary motive for our studies of Vnx1 function was to develop a model system for the biochemical characterization of Type II CAXs including the zebrafish Cax1. Our success in this goal has revealed functional similarities between the Vnx1 and Cax1 proteins. Expression of zebrafish *cax1* in a Δ*vnx1* cells heightened Ca^{2+} accumulation in particular growth conditions indicating that heterologously expressed *cax1* is active. Expression of Cax1 in yeast was also able to restore Ca^{2+}/H^+ exchange activity in nonvacuolar endomembranes, indicating that both proteins can directly mediate Ca^{2+}/H^+ exchange.

Previous studies have implicated intracellular Ca^{2+} signaling in neural crest development (*52*, *53*), and it is well established that propagating Ca^{2+} waves play a crucial role in embryonic development (*18*, *54*−*56*). To our knowledge, however, *cax1* is the first calcium exchanger shown to be specifically required for development of the neural crest. First, *in situ* hybridization studies showed that *cax1* mRNA was specifically expressed in neural crest cells (Figure 5). In addition, *cax1* expression was not detected in morphant embryos in which neural crest development was blocked by inhibiting *tfap2a* and *tfap2c* expression. The detection of *cax1* expression in embryos at 24−48 hpf is also consistent with microarray data that showed transitory *cax1* expression in zebrafish embryos at 24 hpf (Figure 5) (*57*). Second, the reduction in Pax7-expressing cells that we observed in *cax1* morphants (Figure 6) is consistent with the impaired differentiation or survival of neural crest cells. In addition, the defects in jaw cartilage development often arise from perturbations in migration or differentiation of cranial neural crest cells (*58*).

The suppression of *cax1* expression was associated with a transient decrease in pigmentation (Figure 6). Although this reduction in melanocyte formation was short-lived, it was reproducibly observed. We speculate that Cax1 may contribute to the development of pigment-producing cells (melanocytes) via its role in neural crest development (Figure 6). In support of this model, we note that intracellular calcium signaling pathways have been implicated in melanocyte differentiation (*52*, *53*, *59*, *60*). For example, melanocyte cell death was observed in zebrafish mutants (*61*), with reduced activity of a divalent cation channel (*62*). Furthermore, this phenotype can be partially rescued by supplementation with excess calcium (*63*), implicating calcium in melanocyte development and viability.

Our work here reinforces the relationship between intracellular Ca^{2+} and pH in migrating neural crest cells (*64*). The melanosomes are known to undergo a pH shift; early stage melanosomes are relatively acidic but later reach a near-neutral pH (*65*, *66*). Given the membership of Cax1 in the CAX family, it is possible that this transporter provides proton−calcium exchange activity required for pH balance in the neural crest. Interestingly, our experiments indicate that Vnx1, the yeast homologue of Cax1, may also play a role in pH regulation. Yeast cells lacking both the Vnx1 and the Nhx1 endosomal Na^+/H^+ exchanger showed a synthetic growth defect in low pH conditions (Figure 3B), consistent with both these proteins contributing to the regulation of organelle or cytosolic pH. The hygromycin-sensitive phenotype of Δ*vnx1* cells noted in a previous study (*14*) may also reflect altered pH regulation or plasma membrane potential in this mutant.

We have characterized the first CAX from an animal and shown that the transporter plays a critical role in zebrafish development. Future work will define the kinetics of Cax1-mediated Ca^{2+} transport and define the role of Cax1 in Ca^{2+} partitioning and pH homeostasis within the neural crest, which may provide new insights into the evolution of neural crest development in this model vertebrate.

SUPPORTING INFORMATION AVAILABLE

Effect of the vnx1 mutation on sodium, magnesium, potassium and zinc accumulation; manganese content of yeast cells expressing

Vnx1 and Vnx1-HA and Vnx1-YFP; magnesium content of DY1457 cells transformed with pFL44-S (Vector), pFL44YNL (Vnx1), or pFL44YNLHA (Vnx1-HA) grown in standard SC medium supplemented with 10 mM $MgCl_2$; and the gene bank accession numbers used to generate the phylogenetic tree. This material is available free of charge via the Internet at http://pubs.acs.org.

REFERENCES

1. Ashworth, R., and Brennan, C. (2005) Use of transgenic zebrafish reporter lines to study calcium signalling in development. *Briefings Funct. Genomics Proteomics 4*, 186–193.
2. Blader, P., and Strahle, U. (2000) Zebrafish developmental genetics and central nervous system development. *Hum. Mol. Genet. 9*, 945–951.
3. Creton, R. (2004) The calcium pump of the endoplasmic reticulum plays a role in midline signaling during early zebrafish development. *Brain Res. Dev. Brain Res. 151*, 33–41.
4. Cunningham, K. W., and Fink, G. R. (1994) Calcineurin-dependent growth control in Saccharomyces cerevisiae mutants lacking PMC1, a homolog of plasma membrane Ca^{2+} ATPases. *J. Cell Biol. 124*, 351–363.
5. Cheng, N. H., Pittman, J. K., Barkla, B. J., Shigaki, T., and Hirschi, K. D. (2003) The Arabidopsis cax1 mutant exhibits impaired ion homeostasis, development, and hormonal responses and reveals interplay among vacuolar transporters. *Plant Cell 15*, 347–364.
6. Zhao, J., Barkla, B. J., Marshall, J., Pittman, J. K., and Hirschi, K. D. (2008) The Arabidopsis cax3 mutants display altered salt tolerance, pH sensitivity and reduced plasma membrane H^+-ATPase activity. *Planta 227*, 659–669.
7. Kamiya, T., and Maeshima, M. (2004) Residues in internal repeats of the rice cation/H^+ exchanger are involved in the transport and selection of cations. *J. Biol. Chem. 279*, 812–819.
8. Shigaki, T., Rees, I., Nakhleh, L., and Hirschi, K. D. (2006) Identification of three distinct phylogenetic groups of CAX cation/proton antiporters. *J. Mol. Evol. 63*, 815–825.
9. Ivey, D. M., Guffanti, A. A., Zemsky, J., Pinner, E., Karpel, R., Padan, E., Schuldiner, S., and Krulwich, T. A. (1993) Cloning and characterization of a putative Ca^{2+}/H^+ antiporter gene from *Escherichia coli* upon functional complementation of Na^+/H^+ antiporter-deficient strains by the overexpressed gene. *J. Biol. Chem. 268*, 11296–11303.
10. Ohyama, T., Igarashi, K., and Kobayashi, H. (1994) Physiological role of the chaA gene in sodium and calcium circulations at a high pH in Escherichia coli. *J. Bacteriol. 176*, 4311–4315.
11. Miseta, A., Kellermayer, R., Aiello, D. P., Fu, L., and Bedwel, D. M. (1999) The vacuolar Ca^{2+}/H^+ exchanger Vcx1p/Hum1p tightly controls cytosolic Ca^{2+} levels in *S. cerevisiae*. *FEBS Lett. 451*, 132–136.
12. Marchi, V., Sorin, A., Wei, Y., and Rao, R. (1999) Induction of vacuolar Ca^{2+}-ATPase and H^+/Ca^{2+} exchange activity in yeast mutants lacking Pmr1, the Golgi Ca^{2+}-ATPase. *FEBS Lett. 454*, 181–186.
13. Naseem, R., Holland, I. B., Jacq, A., Wann, K. T., and Campbell, A. K. (2008) pH and monovalent cations regulate cytosolic free Ca^{2+} in *E. coli*. *Biochim. Biophys. Acta 1778*, 1415–1422.
14. Cagnac, O., Leterrier, M., Yeager, M., and Blumwald, E. (2007) Identification and characterization of Vnx1p, a novel type of vacuolar monovalent cation/H^+ antiporter of Saccharomyces cerevisiae. *J. Biol. Chem. 282*, 24284–24293.
15. Cai, X., and Lytton, J. (2004) The cation/Ca^{2+} exchanger superfamily: phylogenetic analysis and structural implications. *Mol. Biol. Evol. 21*, 1692–1703.
16. Berridge, M. J. (2004) Calcium signal transduction and cellular control mechanisms. *Biochim. Biophys. Acta 174*, 3–7.
17. Lamason, R. L., Mohideen, M. A., Mest, J. R., Wong, A. C., Norton, H. L., Aros, M. C., Jurynec, M. J., Mao, X., Humphreville, V. R., Humbert, J. E., Sinha, S., Moore, J. L., Jagadeeswaran, P., Zhao, W., Ning, G., Makalowska, I., McKeigue, P. M., O'donnell, D., Kittles, R., Parra, E. J., Mangini, N. J., Grunwald, D. J., Shriver, M. D., Canfield, V. A., and Cheng, K. C. (2005) 2005 SLC24A5, a putative cation exchanger, affects pigmentation in zebrafish and humans. *Science 310*, 1782–1786.
18. Webb, S. E., and Miller, A. L. (2006) Ca^{2+} signaling and early embryonic patterning during the blastula and gastrula periods of zebrafish and *Xenopus* development. *Biochim. Biophys. Acta 1763*, 1192–1208.
19. Bouvard, D., and Block, M. R. (1998) Calcium/calmodulin-dependent protein kinase II controls integrin alpha5beta1-mediated cell adhesion through the integrin cytoplasmic domain associated protein-1alpha. *Biochem. Biophys. Res. Commun. 252*, 46–50.
20. Price, L. S., Langeslag, M., ten Klooster, J. P., Hordijk, P. L., Jalink, K., and Collard, J. G. (2003) Calcium signaling regulates translocation and activation of Rac. *J. Biol. Chem. 278*, 39413–39421.
21. Jin, S. W., Beis, D., Mitchell, T., Chen, J. N., and Stainier, D. Y. (2005) Cellular and molecular analyses of vascular tube and lumen formation in zebrafish. *Development 132*, 5199–5209.
22. Felsenstein, J. (1997) An alternating least squares approach to inferring phylogenies from pairwise distances. *Syst. Biol. 46*, 101–111.
23. Page, R. D. (2002) Visualizing phylogenetic trees using TreeView. Curr. Protoc. Bioinformatics Chapter 6, Unit 6.2.
24. Pittman, J. K., and Hirschi, K. D. (2001) Regulation of CAX1, an Arabidopsis Ca^{2+}/H^+ antiporter. Identification of an N-terminal autoinhibitory domain. *Plant Physiol. 127*, 1020–1029.
25. Eide, D. J., Clark, S., Nair, T. M., Gehl, M., Gribskov, M., Guerinot, M. L., and Harper, J. F. (2005) Characterization of the yeast ionome: a genome-wide analysis of nutrient mineral and trace element homeostasis in *Saccharomyces cerevisiae*. *Genome Biol. 6*, R77.
26. Nass, R., and Rao, R. (1998) Novel localization of a Na^+/H^+ exchanger in a late endosomal compartment of yeast. Implications for vacuole biogenesis. *J. Biol. Chem. 273*, 21054–21060.
27. Nathan, D. F., Vos, M. H., and Lindquist, S. (1999) Identification of SSF1, CNS1, and HCH1 as multicopy suppressors of a *Saccharomyces cerevisiae* Hsp90 loss-of-function mutation. *Proc. Natl. Acad. Sci. U.S.A. 96*, 1409–1414.
28. Bonneaud, N., Ozier-Kalogeropoulos, O., Li, G. Y., Labouesse, M., Minvielle-Sebastia, L., and Lacroute, F. (1991) A family of low and high copy replicative, integrative and single-stranded *S. cerevisiae*/*E. coli* shuttle vectors. *Yeast 7*, 609–615.
29. MacDiarmid, C. W., Milanick, M. A., and Eide, D. J. (2002) Biochemical properties of vacuolar zinc transport systems of *Saccharomyces cerevisiae*. *J. Biol. Chem. 277*, 39187–39194.
30. Sheff, M. A., and Thorn, K. S. (2004) Optimized cassettes for fluorescent protein tagging in *Saccharomyces cerevisiae*. *Yeast 21*, 661–670.
31. Cunningham, K. W., and Fink, G. R. (1996) Calcineurin inhibits VCX1-dependent H^+/Ca^{2+} exchange and induces Ca2+ ATPases in *Saccharomyces cerevisiae*. *Mol. Cell. Biol. 16*, 2226–2237.
32. Longtine, M. S., McKenzie, A., 3rd, Demarini, D. J., Shah, N. G., Wach, A., Brachat, A., Philippsen, P., and Pringle, J. R. (1998) Additional modules for versatile and economical PCR-based gene deletion and modification in *Saccharomyces cerevisiae*. *Yeast 14*, 953–961.
33. Zhao, H., and Eide, D. (1996) The yeast ZRT1 gene encodes the zinc transporter protein of a high-affinity uptake system induced by zinc limitation. *Proc. Natl. Acad. Sci. U.S.A. 93*, 2454–2458.
34. Venema, K., Belver, A., Marin-Manzano, M. C., Rodriguez-Rosales, M. P., and Donaire, J. P. (2003) A novel intracellular K^+/H^+ antiporter related to Na^+/H^+ antiporters is important for K+ ion homeostasis in plants. *J. Biol. Chem. 278*, 22453–22459.
35. Lahner, B., Gong, J., Mahmoudian, M., Smith, E. L., Abid, K. B., Rogers, E. E., Guerinot, M. L., Harper, J. F., Ward, J. M., McIntyre, L., Schroeder, J. I., and Salt, D. E. (2003) Genomic scale profiling of nutrient and trace elements in *Arabidopsis thaliana*. *Nat. Biotechnol. 21*, 1215–1221.
36. Perzov, N., Nelson, H., and Nelson, N. (2000) Altered distribution of the yeast plasma membrane H^+-ATPase as a feature of vacuolar H+-ATPase null mutants. *J. Biol. Chem. 275*, 40088–40095.
37. Sorin, A., Rosas, G., and Rao, R. (1997) PMR1, a Ca^{2+}-ATPase in yeast Golgi, has properties distinct from sarco/endoplasmic reticulum and plasma membrane calcium pumps. *J. Biol. Chem. 272*, 9895–9901.
38. Kimmel, C. B., Ballard, W. W., Kimmel, S. R., Ullmann, B., and Schilling, T. F. (1995) Stages of embryonic development of the zebrafish. *Dev. Dyn. 203*, 253–310.
39. Nasevicius, A., and Ekker, S. C. (2000) Effective targeted gene 'knockdown' in zebrafish. *Nat. Genet. 26*, 216–220.
40. Phillips, B. T., Bolding, K., and Riley, B. B. (2001) *Dev* Zebrafish fgf3 and fgf8 encode redundant functions required for otic placode induction. *Dev. Biol. 235*, 351–365.
41. Robu, M. E., Larson, J. D., Nasevicius, A., Beiraghi, S., Brenner, C., Farber, S. A., and Ekker, S. C. (2007) p53 activation by knockdown technologies. *PLoS Genet. 3*, e78.
42. Solomon, K. S., Kudoh, T., Dawid, I. B., and Fritz, A. (2003) Zebrafish foxi1 mediates otic placode formation and jaw development. *Development 130*, 929–940.

43. Phillips, B. T., Kwon, H. J., Melton, C., Houghtaling, P., Fritz, A., and Riley, B. B. (2006) Zebrafish msxB, msxC and msxE function together to refine the neural-nonneural border and regulate cranial placodes and neural crest development. *Dev. Biol. 294*, 376–390.
44. Cheng, N. H., Pittman, J. K., Shigaki, T., Lachmansingh, J., LeClere, S., Lahner, B., Salt, D. E., and Hirschi, K. D. (2005) Functional association of *Arabidopsis* CAX1 and CAX3 is required for normal growth and ion homeostasis. *Plant Physiol. 138*, 2048–2060.
45. Mei, H., Zhao, J., Pittman, J. K., Lachmansingh, J., Park, S., and Hirschi, K. D. (2007) In planta regulation of the *Arabidopsis* Ca^{2+}/H^{+} antiporter CAX1. *J. Exp. Bot. 58*, 3419–3427.
46. Li, W., and Cornell, R. A. (2007) Redundant activities of Tfap2a and Tfap2c are required for neural crest induction and development of other non-neural ectoderm derivatives in zebrafish embryos. *Dev. Biol. 304*, 338–354.
47. Lacosta, A. M., Canudas, J., Gonzalez, C., Muniesa, P., Sarasa, M., and Dominguez, L. (2007) Pax7 identifies neural crest, chromatophore lineages and pigment stem cells during zebrafish development. *Int J. Dev. Biol. 51*, 327–331.
48. Denis, V., and Cyert, M. S. (2002) Internal Ca^{2+} release in yeast is triggered by hypertonic shock and mediated by a TRP channel homologue. *J. Cell Biol. 156*, 29–34.
49. Strayle, J., Pozzan, T., and Rudolph, H. K. (1999) Steady-state free Ca^{2+} in the yeast endoplasmic reticulum reaches only 10 microM and is mainly controlled by the secretory pathway pump pmr1. *EMBO J. 18*, 4733–4743.
50. Rudolph, H. K., Antebi, A., Fink, G. R., Buckley, C. M., Dorman, T. E., LeVitre, J., Davidow, L. S., Mao, Jl I., and Moir, D. T. (1989) The yeast secretory pathway is perturbed by mutations in PMR1, a member of a Ca^{2+} ATPase family. *Cell 58*, 133–145.
51. Antebi, A., and Fink, G. R. (1992) The yeast Ca^{2+}-ATPase homologue, PMR1, is required for normal Golgi function and localizes in a novel Golgi-like distribution. *Mol. Biol. Cell 3*, 633–65.
52. Wehrle-Haller, B., Meller, M., and Weston, J. A. (2001) Analysis of melanocyte precursors in Nf1 mutants reveals that MGF/KIT signaling promotes directed cell migration independent of its function in cell survival. *Dev. Biol. 232*, 471–483.
53. Evrard, Y. A., Mohammad-Zadeh, L., and Holton, B. (2004) Alterations in Ca^{2+}-dependent and cAMP-dependent signaling pathways affect neurogenesis and melanogenesis of quail neural crest cells in vitro. *Dev. Genes Evol. 214*, 193–199.
54. Ducibella, T., and Fissore, R. (2008) The roles of Ca^{2+}, downstream protein kinases, and oscillatory signaling in regulating fertilization and the activation of development. *Dev. Biol. 315*, 257–279.
55. Ebert, A. M., Hume, G. L., Warren, K. S., Cook, N. P., Burns, C. G., Mohideen, M. A., Siegal, G., Yelon, D., Fishman, M. C., and Garrity, D. M. (2005) Calcium extrusion is critical for cardiac morphogenesis and rhythm in embryonic zebrafish hearts. *Proc. Natl. Acad. Sci. U.S.A. 102*, 17705–17710.
56. Kreiling, J. A., Balantac, Z. L., Crawford, A. R., Ren, Y., Toure, J., Zchut, S., Kochilas, L., and Creton, R. (2008) Suppression of the endoplasmic reticulum calcium pump during zebrafish gastrulation affects left-right asymmetry of the heart and brain. *Mech. Dev. 125*, 396–410.
57. Ouyang, M., Garnett, A. T., Han, T. M., Hama, K., Lee, A., Deng, Y., Lee, N., Liu, H. Y., Amacher, S. L., Farber, S. A., and Ho, S. Y. (2008) A web based resource characterizing the zebrafish developmental profile of over 16,000 transcripts. *Gene Expr. Patterns 8*, 171–180.
58. Kimmel, C. B., Miller, C. T., Kruze, G., Ullmann, B., BreMiller, R. A., Larison, K. D., and Snyder, H. C. (1998) The shaping of pharyngeal cartilages during early development of the zebrafish. *Dev. Biol. 203*, 245–263.
59. Cramer, H., Schmenger, K., Heinrich, K., Horstmeyer, A., Böning, H., Breit, A., Piiper, A., Lundstrom, K., Müller-Esterl, W., and Schroeder, C. (2001) Coupling of endothelin receptors to the ERK/MAP kinase pathway. Roles of palmitoylation and Galphaq. *Eur. J. Biochem. 268*, 5449–5459.
60. Van Raamsdonk, C. D., Fitch, K. R., Fuchs, H., de Angelis, M. H., and Barsh, G. S. (2004) Effects of G-protein mutations on skin color. *Nat. Genet. 36*, 961–968.
61. McNeill, M. S., Paulsen, J., Bonde, G., Burnight, E., Hsu, M. Y., and Cornell, R. A. (2007) Cell death of melanophores in zebrafish trpm7 mutant embryos depends on melanin synthesis. *J. Invest. Dermatol. 127*, 2020–2030.
62. Wei, C., Wang, X., Chen, M., Ouyang, K., Song, L. S., and Cheng, H. (2009) Calcium flickers steer cell migration. *Nature 457*, 901–905.
63. Elizondo, M. R., Arduini, B. L., Paulsen, J., MacDonald, E. L., Sabel, J. L., Henion, P. D., Cornell, R. A., and Parichy, D. M. (2005) Defective skeletogenesis with kidney stone formation in dwarf zebrafish mutant for trpm7. *Curr. Biol. 15*, 667–671.
64. Dickens, C. J., Gillespie, J. I., and Greenwell, J. R. (1990) Measurement of intracellular calcium and pH in avian neural crest cells. *J. Physiol. 428*, 531–544.
65. Watabe, H., Valencia, J. C., Yasumoto, K., Kushimoto, T., Ando, H., Muller, J., Vieira, W. D., Mizoguchi, M., Appella, E., and Hearing, V. J. (2004) Regulation of tyrosinase processing and trafficking by organellar pH and by proteasome activity. *J. Biol. Chem. 279*, 7971–7981.
66. Smith, D. R., Spaulding, D. T., Glenn, H. M., and Fuller, B. B. (2004) The relationship between Na^{+}/H^{+} exchanger expression and tyrosinase activity in human melanocytes. *Exp. Cell Res. 298*, 521–534.